FEBS Letters 589 (2015) 484–489

journal homepage: www.FEBSLetters.org

Structural insights into the catalytic reaction that is involved in the reorientation of Trp238 at the substrate-binding site in GH13 dextran glucosidase

Momoko Kobayashi [a], Wataru Saburi [b], Daichi Nakatsuka [b], Hironori Hondoh [b,1], Koji Kato [a,c], Masayuki Okuyama [b], Haruhide Mori [b], Atsuo Kimura [b], Min Yao [a,c,*]

[a] Graduate School of Life Science, Hokkaido University, Kita-10, Nishi-8, Kita-ku, Sapporo 060-0810, Japan
[b] Research Faculty of Agriculture, Hokkaido University, Kita-9, Nishi-9, Kita-ku, Sapporo 060-8589, Japan
[c] Faculty of Advanced Life Science, Hokkaido University, Kita-10, Nishi-8, Kita-ku, Sapporo 060-0810, Japan

ARTICLE INFO

Article history:
Received 21 November 2014
Revised 5 January 2015
Accepted 5 January 2015
Available online 14 January 2015

Edited by Stuart Ferguson

Keywords:
Retaining glycosidase
Dextran glucosidase
Glycoside hydrolase family 13
Glucosyl-enzyme intermediate
transglucosylation
Acceptor specificity

ABSTRACT

Streptococcus mutans **dextran glucosidase (SmDG) belongs to glycoside hydrolase family 13, and catalyzes both the hydrolysis of substrates such as isomaltooligosaccharides and subsequent transglucosylation to form α-(1 → 6)-glucosidic linkage at the substrate non-reducing ends. Here, we report the 2.4 Å resolution crystal structure of glucosyl-enzyme intermediate of SmDG. In the obtained structure, the Trp238 side-chain that constitutes the substrate-binding site turned away from the active pocket, concurrently with conformational changes of the nucleophile and the acid/base residues. Different conformations of Trp238 in each reaction stage indicated its flexibility. Considering the results of kinetic analyses, such flexibility may reflect a requirement for the reaction mechanism of SmDG.**

1. Introduction

Glycoside hydrolases (GHs), hydrolyzing glycosidic linkages, are widely distributed in the natural world, and play essential roles in the carbohydrate metabolism. In the CAZy database, GHs are classified into 133 families based on sequence similarity (http://www.cazy.org) [1]. Among GH families, GH family 13 (GH13) contains a large variety of enzymes, such as α-amylase (EC 3.2.1.1), cyclodextrin glucanotransferase (CGTase, EC 2.4.1.19), and α-glucosidase (EC 3.2.1.20), and is further segmented into 40 subfamilies (represented as GH13_x) [2]. GH13 enzymes are structurally related to enzymes in GH70 and 77, which form clan GH-H, the so-called α-amylase family. α-Amylase-family enzymes catalyze the reaction through a double displacement mechanism including glycosylation and deglycosylation steps [3]. In the glycosylation step, a catalytic nucleophile attacks the anomeric carbon of glycosyl residue bound to subsite −1, and general acid/base catalyst donates a proton to the glycosidic oxygen. Via high-energy oxocarbenium ion-like transition state, aglycone is released and β-glycosyl-enzyme intermediate is formed. In the following deglycosylation step, an acceptor molecule, activated by the dissociated acid/base, attacks C1 of glucosyl residue of the intermediate, and the glycone part is released with an anomeric inversion. Water and sugar molecules serve as acceptor molecules in hydrolysis and ransglucosylation, respectively. Among clan GH-H enzymes, structures of covalent-bond intermediates are available for the following enzymes: CGTase [4], amylosucrase (AS, EC 2.4.1.4, GH13_4) [5], sucrose phosphorylase (EC 2.4.1.7, GH13_18) [6], glycogen-debranching enzyme TreX (EC 2.4.1.25 and EC 3.2.1.68, GH13_11) [7], α-amylase (GH13_24) [8], and amylomaltase (EC 2.4.1.25, GH77) [9]. Some of these enzymes change the conformation of amino acid residues surrounding the active site during the

Abbreviations: AS, amylosucrase; α-GF, α-glucosyl fluoride; BSA, bovine serum albumin; CGTase, cyclodextrin glucanotransferase; GH, glycoside hydrolase; HPAEC-PAD, high performance anion exchange chromatography with pulsed amperometric detection; O16G, oligo-1,6-glucosidase; pNPG, *p*-nitrophenyl α-glucopyranoside; SmDG, *Streptococcus mutans* dextran glucosidase; TVAI, *Thermoactinomyces vulgaris* R-47 α-amylase 1; TVAII, *T. vulgaris* R-47 α-amylase 2

* Corresponding author.
[1] Current affiliation: Graduate School of Biosphere Science, Hiroshima University, Higashi-Hiroshima 739-8528, Japan.

http://dx.doi.org/10.1016/j.febslet.2015.01.005

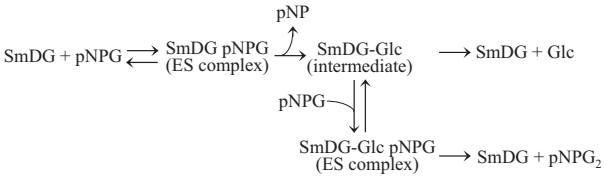

Fig. 1. Kinetic scheme of SmDG reactions. SmDG-Glc, the glucosyl-enzyme intermediate. Glc, pNP, and $pNPG_2$ represent glucose, *p*-nitrophenol, and *p*-nitrophenyl isomaltoside, respectively.

formation of an intermediate. Thus, a precise catalytic mechanism could be inferred from the structure of glycosyl-enzyme intermediate.

Streptococcus mutans dextran glucosidase (SmDG, EC 3.2.1.70) hydrolyzes α-(1 → 6)-glucosidic linkage at the non-reducing ends of substrates to liberate α-glucose [10], and belongs to GH13_31, together with oligo-1,6-glucosidase (O16G, EC 3.2.1.10), α-glucosidase, and isomaltulose synthase (EC 5.4.99.11). SmDG prefers isomaltooligosaccharides, as does O16G, but has higher activity with long-chain substrates, such as dextran, than O16G [10,11]. At high substrate concentrations, SmDG also catalyzes transglucosylation to form α-(1 → 6) linkage. We have analyzed kinetics of the SmDG reaction, in which hydrolysis and transglucosylation occur simultaneously, and proposed a kinetic model (Fig. 1) [12]. In this model, K_{TG} parameter (substrate concentration giving 50% of transglucosylation ratio) is defined for evaluating transglucosylation activity. The crystal structures of SmDG wild-type and isomaltotriose complex have been reported [13]. In the wild-type structure, Tris and glycerol bind to subsite −1 and +1, respectively. No significant conformational difference was observed between these structures. In isomaltotriose complex, isomaltotriose occupied subsites from −1 to +2, forming Michaelis complex. In the substrate-binding site, Trp238 is involved in the formation of +1/+2 subsites. Mutational analysis of this residue showed that Trp238 is important for both high preference for long-chain substrate and transglucosylation [11].

In this study, we investigated the structure of the glucosyl-enzyme intermediate of acid/base mutant SmDG (E236Q) to elucidate the precise reaction mechanism. The E236Q and a substrate with good leaving group, α-glucosyl fluoride (α-GF) were used to trap the intermediate. In the glycosylation step, a good leaving group aglycone from α-GF does not require the protonic assistance of the general acid. The breakdown of covalent-bond intermediate is severely prevented by the substitution of the general base, which normally activates a water or sugar molecule by abstracting a proton in the deglycosylation step [5]. In the intermediate structure, conformational change of Trp238 side-chain was observed. The role of this conformational change was discussed based on structural comparison and kinetic analysis.

2. Materials and methods

2.1. Preparation of wild-type and variant SmDGs

We performed site-directed mutagenesis using the QuikChange technique, or the megaprimer PCR method [14] as described previously [11]; we used the wild-type expression plasmid [11] as a template and primers shown in Table 1. Amplified DNA fragment was cloned into pET23d (Merck, Darmstadt, Germany) as described previously [11]. The wild-type and variant SmDGs were produced in *Escherichia coli* BL21 (DE3) CodonPlus-RIL cells (Agilent Technologies, Santa Clara, CA) and purified by Ni-chelating column chromatography as described previously [15]. The samples were dialyzed against 20 mM sodium acetate buffer (pH 6.0), and stored

Table 1
Sequences of the primers for producing SmDG variants.

Name	Sequence (5′ → 3′)
E236Qs	GTGGGG CAA ACTTGGGGAGCAACGCCT
E236Qa	CCAAGT TTG CCCCACAGTCAGCAGATC
F262As	TGGTTTTTCAA GCT GAACATATTGG
F262Ws	TGGTTTTTCAA TGG GAACATATTGG

Substituted nucleotides are underlined. s, sense; a, antisense.

at 4 °C. E236Q was purified using Ni-chelating column chromatography followed by gel filtration column chromatography (HiLoad 16/600 Superdex 200 pg; GE Healthcare, Uppsala, Sweden) in 20 mM sodium acetate buffer (pH 6.0) containing 500 mM NaCl. Purified E236Q was dialyzed against 10 mM sodium acetate buffer (pH 6.0) and concentrated for crystallization (to 22 mg/mL) using Amicon Ultra-15 10K centrifugal filter devices (Merck).

2.2. Crystallization and data collection

Crystallization was performed by the sitting-drop vapor diffusion method at 20 °C, in which 2.5 μL of E236Q solution (22 mg/mL) and equivalent volume of reservoir solution were mixed. The crystals of E236Q glucosyl-enzyme intermediate were obtained by co-crystallization with 5 mM α-GF [16] in drops under the condition of 100 mM Tris–HCl (pH 7.5), 200 mM calcium chloride and 18% (w/v) polyethylene glycol (PEG) 6000. The ligand-free E236Q crystals were grown by using reservoir solution of 100 mM sodium 4-(2-hydroxyethyl)-1-piperazineethanesulfonic acid (pH 7.4), 200 mM calcium chloride and 18% (w/v) PEG 6000. For data collection at 100 K, the intermediate crystal was soaked in reservoir solution supplemented with 25% (v/v) glycerol and 5 mM α-GF, while the ligand-free E236Q crystal was soaked in paratone-N. Diffraction data of the intermediate and ligand-free E236Q were collected at beamline BL-38B1 of SPring-8 (Hyogo, Japan) and BL-17A of Photon Factory (Ibaraki, Japan), respectively. All data sets were processed using the *XDS* program suite [17]. Data collection statistics are summarized in Table 2.

2.3. Structure determination and refinement

Structures of glucosyl-enzyme intermediate and ligand-free E236Q was determined by rigid-body refinement using the structure of isomaltotriose complex (PDB: 2ZID) as an initial model. Several rounds of refinement were performed using the program *Phenix.refine* in the *Phenix* program suite [18], alternated with manual fitting and rebuilding based on $2F_o - F_c$ and $F_o - F_c$ electron densities using *COOT* [19]. The final refinement statistics and geometry defined by *MolProbity* [20] are summarized in Table 2.

2.4. Analysis of transglucosylation products

A reaction solution (300 μL) containing 7.8 nM SmDG, 25 mM α-GF, 25 mM glucose or maltose, 0.2 mg/mL bovine serum albumin (BSA), and 0.1 M sodium phosphate buffer (pH 6.0), was incubated at 37 °C. Samples (40 μL) were taken at 15, 30, 60, 90, and 120 min, and desalted with ion-exchange resin (Amberlite MB-4, Dow Chemical, Midland, MI). A 1-μL aliquot of the sample was immediately applied to TLC Silica gel 60 plate (Merck). The chromatography was repeated twice using 2-propanol/1-butanol/water (2:2:1, v/v/v). Sugars were visualized by spraying the detection reagent (anisaldehyde:sulfuric acid:acetic acid = 1:2:100, v/v/v) and heating the plate at 120 °C. The reaction mixture, prepared as described above (reaction was stopped at 100 °C for 10 min), was quantitatively analyzed by high performance anion exchange chromatogra-

Table 2
X-ray data collections and refinement statistics.

	SmDG E236Q	SmDG E236Q Glucosyl-enzyme intermediate
Data collection		
Synchrotron	Photon Factory	SPring-8
Beamline	BL-17A	BL-38B1
Wavelength (Å)	0.9800	1.0000
Space group	$P2_12_12_1$	$P2_12_12_1$
Unit cell parameters		
a, *b*, *c* (Å)	72.2, 82.6, 103.6	73.0, 83.4, 103.8
Resolution range (Å)	50.00–2.09 (2.22–2.09)	50.00–2.40 (2.55–2.40)
[a]R_{merge}	0.088 (0.345)	0.152 (0.781)
Redundancy	5.84 (5.10)	5.39 (5.42)
Completeness (%)	99.4 (97.4)	99.6 (99.4)
Number of unique reflections	36936 (5771)	25354 (4008)
$I/\sigma(I)$	14.81 (4.45)	10.86 (2.23)
Refinenment		
Resolution (Å)	48.11–2.09	44.11–2.40
R_{work}/[b]R_{free} (%)	17.94/21.90	21.73/26.28
Atoms		
Protein	4373	4373
Glucose	0	11
Glycerol	0	12
Water	353	186
Calcium ion	4	3
[c]P6G	19	0
Ramachandran (%)		
Favored	96.44	94.38
Allowed	3.56	5.24
Outliers	0	0.37
Mean *B*-factor (Å^2)		
Average	25.5	36.9
Protein	25.2	36.9
Ligands	31.6	36.6
Water	28.1	37.7
RMSD		
Bond lengths (Å)	0.003	0.003
Bond angles (°)	0.704	0.675

[a] $R_{merge} = \Sigma_{hkl}\Sigma_i|I_i(hkl) - \langle I_i(hkl)\rangle|/\Sigma_{hkl}\Sigma_i I_i(hkl)$, where i is the number of observations of a given reflection and $I_i(hkl)$ is the average of the i observations.
[b] R_{free} was calculated with a 5% fraction of randomly selected reflections evaluated from refinement. The highest resolution shell is shown in parentheses.
[c] P6G is hexaethylene glycol.

phy with pulsed amperometric detection (HPAEC-PAD). Samples that were appropriately diluted were injected onto CarboPac PA1 column (Dionex, Sunnyvale, CA) and eluted with 200 mM NaOH at a flow rate of 0.8 mL/min.

2.5. Kinetic analysis of transglucosylation by SmDG variants

Transglucosylation activity of SmDG variants was analyzed using *p*-nitrophenyl α-glucopyranoside (pNPG; Nacalai Tesque, Kyoto, Japan) and isomaltose (Tokyo Chemical Industry, Tokyo, Japan) as substrates. In the reaction with pNPG, K_{TG} values were determined as described elsewhere (Fig. 1) [12]. With isomaltose, transglucosylation ratios were measured at 12 mM substrate concentration. The reaction mixture (250 μL) containing an adequate concentration of enzyme, 12 mM isomaltose, 40 mM sodium acetate buffer (pH 6.0), and 0.2 mg/mL BSA, was incubated at 37 °C. At 5, 10, 15, and 20 min, samples (50 μL) were withdrawn and heated at 100 °C for 10 min to stop the reaction. Product concentrations were measured by HPAEC-PAD as described above. Transglucosylation and hydrolysis of isomaltose are illustrated in the following schematic diagram.

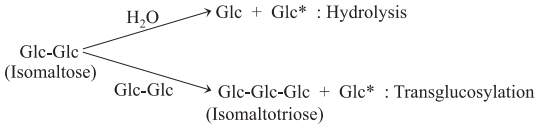

where Glc and Glc* are glucose and glucose of aglycone-side, respectively. Reaction velocities for aglycone release (v_{ag}), hydrolysis (v_h), and transglucosylation (v_{TG}) were calculated using the following Eqs. (1)–(3), in which v_{Glc} and v_{IG3} are the velocities for liberation of glucose and isomaltotriose, respectively.

$$v_{TG} = v_{IG3} \quad (1)$$

$$v_h = (v_{Glc} - v_{IG3})/2 \quad (2)$$

$$v_{ag} = v_{Glc} - v_h (= v_h + v_{IG3}) \quad (3)$$

The transglucosylation ratio was calculated as follows

$$\text{Transglucosylation ratio } (\%) = v_{TG}/v_{ag} \times 100 \quad (4)$$

3. Results and discussion

3.1. The structures of glucosyl-enzyme intermediate and ligand-free E236Q

The structure of the acid/base mutant of SmDG (E236Q), covalently bound to glucose, was determined at 2.4 Å resolution (PDB: 4WLC). Overall structure was almost identical to that of SmDG wild-type (PDB: 2ZIC) and isomaltotriose complex (PDB: 2ZID) with r.m.s.d (root-mean-square deviation) values of 0.27 and 0.26 Å for main-chain, respectively. Clear electron density maps of two ligands were observed in the active site of intermediate structure (Fig. 2A). The first ligand was a glycerol molecule, a component of the cryoprotectant. This molecule was bound to subsite +1 correspondingly to a glycerol molecule bound to wild-type [13]. The other was β-glucose bound to subsite −1. The electron density map unambiguously showed the covalent bond between C1 of glucose and OD2 of the nucleophile Asp194 at the distance of 1.48 Å. In comparison with the corresponding atoms in the isomaltotriose complex, C1 of glucose shifted 1.27 Å toward Asp194 to form the covalent bond, and Asp194 also moved toward glucose (Fig. 2B). These conformational changes in subsite −1 were also observed in the structures of AS [5]. In the SmDG intermediate, main-chain of β → α loop 4 including Asp194 shifted compared with the corresponding loops of other SmDG structures (Fig. 2B). The glucose moiety of the intermediate took $^4C_1$ chair conformation, slightly more stable than the corresponding glucosyl residue in isomaltotriose complex. C2–C1–O5–C5 torsion angles of glucosyl residues in subsite −1 of the intermediate and isomaltotriose complex were −60° and −57°, respectively. Stabilization of the glucosyl residue in subsite −1 through the formation of the intermediate has been observed in several related enzymes [4,5,8,9]. Two other structural features stabilizing the intermediate, found in GH77 amylomaltase, were also observed in SmDG. Firstly, the plane of the ester bond with Asp194 and C1 of glucose was perpendicular to the plane of the glucose ring. Barends and coworkers have suggested that this perpendicular orientation stabilized the intermediate shielding of C1 from a nucleophilic attack by an acceptor [9]. Secondly, the acid/base rotated and shifted slightly from the cleavage site to avoid proximity to OD1 of the nucleophile. NE2 and OE1 of Gln236 of the intermediate were 3.70 and 4.41 Å, respectively, from the glucosidic oxygen of superposed isomaltotriose, whereas the distance between NE2 of Gln236 and glucosidic oxygen was 3.14 Å in isomaltotriose complex. The conformations of residues forming subsite −1 except Asp194 and

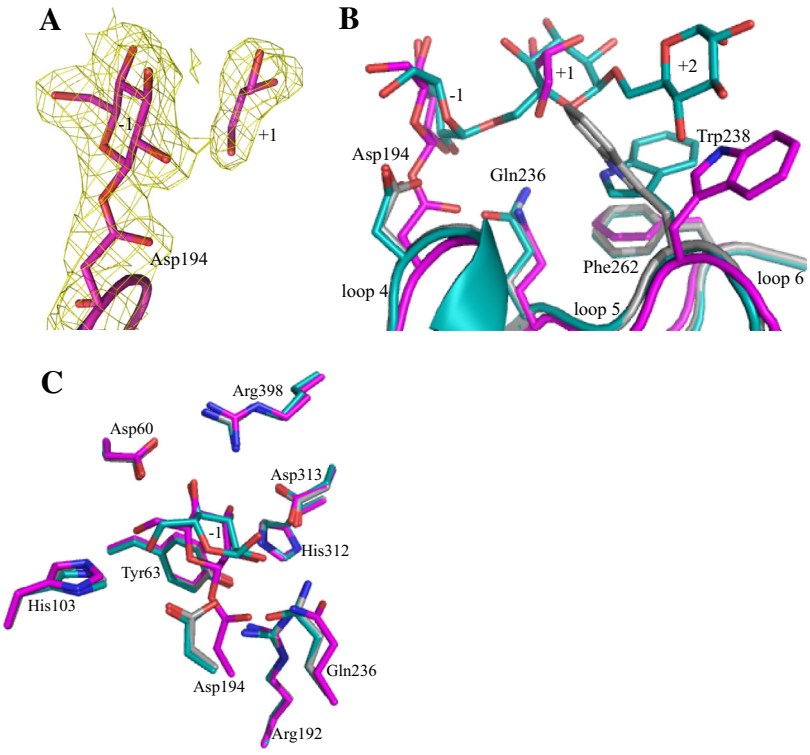

Fig. 2. Structural details of SmDG active site. (A) $2F_o - F_c$ map for ligands bound to the active site and Asp194 is drawn in yellow. The electron density is contoured at 1 σ. Glucose and glycerol molecules bind to subsites −1 and +1, respectively. (B) Comparison between the structures of ligand-free E236Q, isomaltotriose complex, and covalent-bond intermediate. Main chains of proteins are represented by cartoon. β → α loop 4, 5, and 6 of domain A are shown. (C) Side-chains of amino acid residues within 3-Å distance from glucose in subsite −1. In (A–C), the side-chains of amino acid residues and ligands are shown in stick representation, with O and N atoms colored red and blue. The ligand-free E236Q, isomaltotriose complex, and covalent-bond intermediate are in gray, dark cyan, and magenta, respectively. Variations and residue numbers are also shown. Subsite numbers are shown as −1 to +2. All figures were produced using Pymol [29].

Gln236 did not differ from those in other SmDG structures (Fig. 2C).

The formation of the intermediate caused a remarkable conformational change of the indole ring of Trp238, which is on β → α loop 5 and is involved in subsites +1 and +2 in isomaltotriose complex [13]. NE1 of Trp238 formed a hydrogen bond with NE2 of the acid/base Gln236 at a distance of 3.27 Å in the isomaltotriose complex. In contrast, Trp238 in the intermediate turned away from the active pocket concurrently with conformational changes of the nucleophile Asp194 and acid/base Glu (Gln) 236 (open form, Fig. 2B). The nucleophile Asp194 forms covalent bond with glucose, the acid/base Glu (Gln) 236 side-chain rotates to avoid the crush with Asp194, and hydrogen bond between the acid/base and Trp238 is disrupted. The main-chain of β → α loop 5 also changed the conformation. *B*-factor values of Trp238 side-chain in the intermediate were high (53.4–64.4 Å^2) comparing to the total average value of 36.9 Å^2, indicating the flexibility of Trp238 in the open form. To verify the conformational change of Trp238, the structure of ligand-free E236Q was also revealed at 2.1 Å resolution (PDB: 4XB3). In this structure, Trp238 side-chain showed the different conformation from others, although overall structure was almost identical to that of wild-type and isomaltotriose complex with r.m.s.d values of 0.20 and 0.17 Å for main-chain atoms, respectively (Fig. 2B). Such different conformations of Trp238 in each reaction stage indicate its flexibility.

3.2. Acceptor specificity of wild-type SmDG

Structural analysis of SmDG suggested that Trp238 took the open form in the intermediate, whereas it assumes the closed form to make subsites +1 and +2 in the Michaelis complex (Fig. 2B). Trp238 does not interact with the substrate at subsite +1 and has a steric hindrance at subsite +2 in the open form. Thus, it could not easily accept sugars during transglucosylation while remaining in the open form. To evaluate the conformation of Trp238 in the deglycosylation step of transglucosylation, acceptor specificity of wild-type SmDG was investigated using glucose and maltose as acceptors (Fig. 3). α-GF, having a good leaving group, was used as a donor substrate. Glucose and maltose served as acceptor substrates, and isomaltose and panose were obtained as transglucosylation products, respectively. α-GF was not used as acceptor and the spot of such product did not appear. In the later stage of the reaction with maltose, small amounts of isomaltose was produced from glucose, which was accumulated because of the hydrolysis of

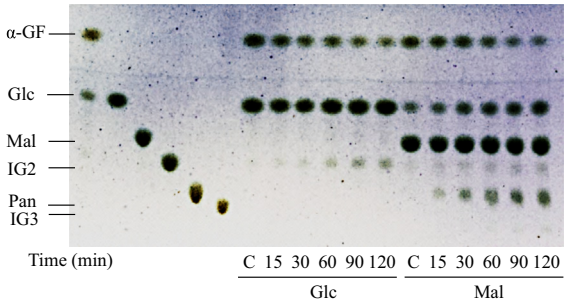

Fig. 3. Time course of wild-type SmDG reaction with α-GF and two acceptors. Transglucosylation products with α-GF and glucose or maltose were measured by TLC. Reaction time and acceptor sugars are shown below the chromatogram. The first six lanes are standard sugars. Glc, glucose; Mal, maltose; IG2, isomaltose; Pan, panose; IG3, isomaltotriose. C, control: BSA was used instead of the enzyme.

α-GF and panose. In the early stage of the reaction, release rates of isomaltose and panose were 58.3 and 225 s^{-1}, respectively. The finding that both a monosaccharide and disaccharide could be acceptor substrates suggested that Trp238 returned to the closed form in the deglycosylation step of transglucosylation.

3.3. The effect of the alteration in Trp238 flexibility on transglucosylation

Previous study has shown that Trp238 affects transglucosylation [11]. The analysis of acceptor specificity described above, indicates that the flexibility of Trp238 might be important for transglucosylation. To assess the effect of changes on Trp238 flexibility for transglucosylation, we performed mutant analysis of Phe262 which is the only residue interacted with Trp238 by aromatic stacking except for Glu (Gln) 236 (Fig. 2B). Considering hydrophobic interaction of Phe262 with around residues, especially the aromatic stacking interaction with Trp238, Ala or Trp was selected for substitution in order to change the flexibility of Trp238. Transglucosylation activity of the mutant enzymes with pNPG and isomaltose was investigated (Table 3). F262A/W mutant enzymes showed lower activity with both substrates than the wild-type enzyme. The K_{TG} value (calculated from release rates of transglucosylation products at 0.2–12 mM pNPG) of F262A was about a seventh of the wild-type. However, K_{TG} of F262W showed a 1.2-fold increase in comparison with the wild-type. These results suggest that F262A has a stronger and F262W has a weaker preference for transglucosylation than that of the wild-type enzyme. These tendencies are consistent with the results for isomaltose. The transglucosylation ratios of F262A, F262W, and wild-type for 12 mM isomaltose were 84.0%, 6.43%, and 25.9%, respectively. These results might reflect the flexibility of Trp238 in each enzyme. In F262A, Trp238 could be more flexible than which in the wild-type and easy to form the open conformation. On the other hand, in F262W, the flexibility of Trp238 would be lower than the wild-type because of enhanced stacking interaction. Taken all results together, it is suggested that a high flexibility of Trp238 side-chain is important for transglucosylation.

3.4. Structural insights into catalytic reaction involving reorientation of Trp238

Structural analyses of SmDG suggested the conformational changes of Asp194, Glu (Gln) 236, and Trp238 during reaction (Fig. 4). The conformation of flexible Trp238 in the ligand-free structure changes to the closed form by the binding of substrate to form ES complex. In isomaltotriose complex, closed formed Trp238 is stabilized by hydrogen bond with Glu (Gln) 236 and stacking interaction with Phe262 for substrate binding. When aglycone is released and the covalent-bond intermediate is formed, the orientation of Trp238 side-chain changed to the open form concurrently with conformational changes of Asp194 and Glu236.

Table 3
Aglycone-releasing velocity and transglucosylation activity of SmDG wild-type and Phe262 mutants.

	pNPG		Isomaltose	
	v_{ag} (s^{-1})	K_{TG} (mM)	v_{ag} (s^{-1})	TG ratio (%)
Wild type	196	1.03	305	25.9
F262A	6.36	0.158	5.42	84.0
F262W	29.5	1.23	1.43	6.43

pNPG and isomaltose were used as substrates. v_{ag} were aglycone-releasing rate on 2 mM pNPG or 12 mM isomaltose. K_{TG} on pNPG were calculated as described [12]. K_{TG} value of wild type was quoted from the previous report [12]. Transglucosylation (TG) ratio on 12 mM isomaltose were calculated according to Eqs. (1)–(4).

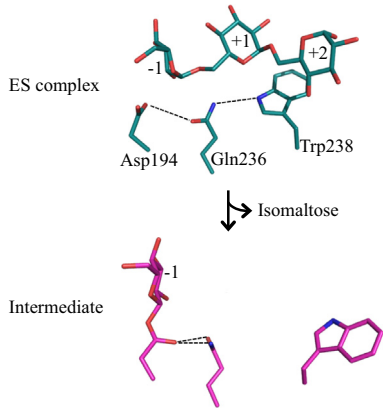

Fig. 4. Conformational changes of active site of SmDG during reaction on isomaltotriose. The conformational change of three amino acid residues between isomaltotriose complex (ES complex) and the covalent-bond intermediate was shown. Hydrogen bonds were represented as dashed lines. Other representation is corresponding to Fig. 2.

Structural superposition of the intermediate and isomaltotriose complex suggests that Trp238 of intermediate SmDG does not contact with the substrate in subsite +1, and crushes with O4 of the glucose bound to subsite +2. Considering the result of acceptor specificity analysis, Trp238 might need to return to the closed form in the deglycosylation step of transglucosylation for binding acceptor, as the conformation in isomaltotriose complex (isomaltose is acceptor). Such reorientation of Trp238 to the closed form could make the covalent bond of the intermediate unstable and facilitate the deglycosylation step. Taken the conformations of active site in the ligand-free, isomaltotriose complex, and intermediate into consideration, deglycosylation reaction of hydrolysis might proceed without returning to the closed form.

Comparisons of amino acid sequences show that many GH13 enzymes possess Trp residues corresponding to Trp238 in SmDG. The Trp is highly conserved in GH13_20 members, including neopullulanases (EC 3.2.1.135), cyclomaltodextrinases (EC 3.2.1.54), and maltogenic amylases (EC 3.2.1.133), and in GH13_36 members such as α-amylases [21]. The Trp residue is important for substrate binding at subsite +2 in *Thermoactinomyces vulgaris* R-47 α-amylase 1 (TVAI, GH13_21) and α-amylase 2 (TVAII, GH13_20), *Geobacillus stearothermophilus* neopullulanase (GH13_20), and *Halothermothrix orenii* α-amylase (GH13_36) [22–27]. Two orientation patterns of the Trp side-chain are observed in GH13 enzymes with known structures. (1) As observed in SmDG, the N atom of indole forms a hydrogen bond. Trp residues of TVAI and TVAII assume this orientation [22–24,28]. TVAI and TVAII also have hydrogen-bond networks involving the nucleophile, the acid/base, and the Trp residue [24,28], and possibly rearrange this residue during the formation of the intermediate, correspondingly to SmDG. (2) The Trp residue and the acid/base have no hydrogen-bond contact. In *G. stearothermophilus* neopullulanase and *H. orenii* α-amylase, the rings of the Trp residues are turned over in comparison with the orientation in SmDG-type enzymes [25,26]. It is unclear whether the Trp residue of this type also changes its orientation during the reaction.

In this study, we found that the structural rearrangement of the active site of SmDG was triggered by the formation of the glucosyl-enzyme intermediate. The flexibility of Trp238 side-chain would be important for reaction mechanism of SmDG.

Acknowledgments

We thank the staffs of beamline BL-38B1 at SPring-8 and beamline BL-17A at Photon Factory. A part of this work was supported

by Grants-in-Aid for Scientific Research from the Japan Society for the Promotion of Science (Grant Number, 24 871) and Platform for Drug Discovery, Informatics, and Structural Life Science from the Ministry of Education, Culture, Sports, Science, and Technology, Japan.

References

[1] Cantarel, B.L., Coutinho, P.M., Rancurel, C., Bernard, T., Lombard, V. and Henrissat, B. (2009) The Carbohydrate-Active EnZymes database (CAZy): an expert resource for Glycogenomics. Nucleic Acids Res. 37, D233–238.
[2] Stam, M.R., Danchin, E.G., Rancurel, C., Coutinho, P.M. and Henrissat, B. (2006) Dividing the large glycoside hydrolase family 13 into subfamilies: towards improved functional annotations of α-amylase-related proteins. Protein Eng. Des. Sel. 19, 555–562.
[3] Rye, C.S. and Withers, S.G. (2000) Glycosidase mechanisms. Curr. Opin. Chem. Biol. 4, 573–580.
[4] Uitdehaag, J.C., Mosi, R., Kalk, K.H., van der Veen, B.A., Dijkhuizen, L., Withers, S.G. and Dijkstra, B.W. (1999) X-ray structures along the reaction pathway of cyclodextrin glycosyltransferase elucidate catalysis in the α-amylase family. Nat. Struct. Biol. 6, 432–436.
[5] Jensen, M.H., Mirza, O., Albenne, C., Remaud-Simeon, M., Monsan, P., Gajhede, M. and Skov, L.K. (2004) Crystal structure of the covalent intermediate of amylosucrase from *Neisseria polysaccharea*. Biochemistry 43, 3104–3110.
[6] Mirza, O., Skov, L.K., Sprogøe, D., van den Broek, L.A., Beldman, G., Kastrup, J.S. and Gajhede, M. (2006) Structural rearrangements of sucrose phosphorylase from *Bifidobacterium adolescentis* during sucrose conversion. J. Biol. Chem. 281, 35576–35584.
[7] Woo, E.J., Lee, S., Cha, H., Park, J.T., Yoon, S.M., Song, H.N. and Park, K.H. (2008) Structural insight into the bifunctional mechanism of the glycogen-debranching enzyme TreX from the archaeon *Sulfolobus solfataricus*. J. Biol. Chem. 283, 28641–28648.
[8] Zhang, R., Li, C., Williams, L.K., Rempel, B.P., Brayer, G.D. and Withers, S.G. (2009) Directed "*in situ*" inhibitor elongation as a strategy to structurally characterize the covalent glycosyl-enzyme intermediate of human pancreatic α-amylase. Biochemistry 48, 10752–10764.
[9] Barends, T.R., Bultema, J.B., Kaper, T., van der Maarel, M.J., Dijkhuizen, L. and Dijkstra, B.W. (2007) Three-way stabilization of the covalent intermediate in amylomaltase, an α-amylase-like transglycosylase. J. Biol. Chem. 282, 17242–17249.
[10] Russell, R.R. and Ferretti, J.J. (1990) Nucleotide sequence of the dextran glucosidase (*dexB*) gene of *Streptococcus mutans*. J. Gen. Microbiol. 136, 803–810.
[11] Saburi, W., Mori, H., Saito, S., Okuyama, M. and Kimura, A. (2006) Structural elements in dextran glucosidase responsible for high specificity to long chain substrate. Biochim. Biophys. Acta 1764, 688–698.
[12] Kobayashi, M., Hondoh, H., Mori, H., Saburi, W., Okuyama, M. and Kimura, A. (2011) Calcium ion-dependent increase in thermostability of dextran glucosidase from *Streptococcus mutans*. Biosci. Biotechnol. Biochem. 75, 1557–1563.
[13] Hondoh, H., Saburi, W., Mori, H., Okuyama, M., Nakada, T., Matsuura, Y. and Kimura, A. (2008) Substrate recognition mechanism of α-1,6-glucosidic linkage hydrolyzing enzyme, dextran glucosidase from *Streptococcus mutans*. J. Mol. Biol. 378, 913–922.
[14] Datta, A.K. (1995) Efficient amplification using 'megaprimer' by asymmetric polymerase chain reaction. Nucleic Acids Res. 23, 4530–4531.
[15] Saburi, W., Kobayashi, M., Mori, H., Okuyama, M. and Kimura, A. (2013) Replacement of the catalytic nucleophile aspartyl residue of dextran glucosidase by cysteine sulfinate enhances transglycosylation activity. J. Biol. Chem. 288, 31670–31677.
[16] Hayashi, M., Hashimoto, S. and Noyori, R. (1984) Simple synthesis of glycosyl fluorides. Chem. Lett., 1747–1750
[17] Kabsch, W. (2010) XDS. Acta Crystallogr. Sect. D 66, 125–132.
[18] Adams, P.D., Afonine, P.V., Bunkoczi, G., Chen, V.B., Davis, I.W., Echols, N., Headd, J.J., Hung, L.W., Kapral, G.J., Grosse-Kunstleve, R.W., McCoy, A.J., Moriarty, N.W., Oeffner, R., Read, R.J., Richardson, D.C., Richardson, J.S., Terwilliger, T.C. and Zwart, P.H. (2010) PHENIX: a comprehensive Python-based system for macromolecular structure solution. Acta Crystallogr. Sect. D 66, 213–221.
[19] Emsley, P. and Cowtan, K. (2004) Coot: model-building tools for molecular graphics. Acta Crystallogr. Sect. D 60, 2126–2132.
[20] Chen, V.B., Arendall 3rd, W.B., Headd, J.J., Keedy, D.A., Immormino, R.M., Kapral, G.J., Murray, L.W., Richardson, J.S. and Richardson, D.C. (2010) MolProbity: all-atom structure validation for macromolecular crystallography. Acta Crystallogr. Sect. D 66, 12–21.
[21] Majzolvá, K., Pukajová, Z. and Janeček, Š. (2013) Tracing the evolution of the α-amylase subfamily GH13_36 covering the amylolytic enzymes intermediate between oligo-1,6-glucosidases and neopullulanases. Carbohydr. Res. 367, 48–57.
[22] Abe, A., Tonozuka, T., Sakano, Y. and Kamitori, S. (2004) Complex structures of *Thermoactinomyces vulgaris* R-47 α-amylase 1 with malto-oligosaccharides demonstrate the role of domain N acting as a starch-binding domain. J. Mol. Biol. 335, 811–822.
[23] Ohtaki, A., Mizuno, M., Tonozuka, T., Sakano, Y. and Kamitori, S. (2004) Complex structures of *Thermoactinomyces vulgaris* R-47 α-amylase 2 with acarbose and cyclodextrins demonstrate the multiple substrate recognition mechanism. J. Biol. Chem. 279, 31033–31040.
[24] Ohtaki, A., Mizuno, M., Yoshida, H., Tonozuka, T., Sakano, Y. and Kamitori, S. (2006) Structure of a complex of *Thermoactinomyces vulgaris* R-47 α-amylase 2 with maltohexaose demonstrates the important role of aromatic residues at the reducing end of substrate binding cleft. Carbohydr. Res. 341, 1041–1046.
[25] Hondoh, H., Kuriki, T. and Matsuura, Y. (2003) Three-dimensional structure and substrate binding of *Bacillus stearothermophilus* neopullulanase. J. Mol. Biol. 326, 177–188.
[26] Sivakumar, N., Li, N., Tang, J.W., Patel, B.K. and Swaminathan, K. (2006) Crystal structure of AmyA lacks acidic surface and provide insights into protein stability at poly-extreme condition. FEBS Lett. 580, 2646–2652.
[27] Ohtaki, A., Iguchi, A., Mizuno, M., Tonozuka, T., Sakano, Y. and Kamitori, S. (2003) Mutual conversion of substrate specificities of *Thermoactinomyces vulgaris* R-47 α-amylases TVAI and TVAII by site-directed mutagenesis. Carbohydr. Res. 338, 1553–1558.
[28] Abe, A., Yoshida, H., Tonozuka, T., Sakano, Y. and Kamitori, S. (2005) Complexes of *Thermoactinomyces vulgaris* R-47 α-amylase 1 and pullulan model oligosaccharides provide new insight into the mechanism for recognizing substrates with α-(1,6) glycosidic linkages. FEBS J. 272, 6145–6153.
[29] DeLano, W.L. (2002) The PyMOL Molecular Graphics System, DeLano Scientific, Palo Alto, CA.